IBRACON Structures and Materials Journal
Revista IBRACON de Estruturas e Materiais
ISSN 1983-4195 ismj.org

ORIGINAL ARTICLE

Short columns composed of concrete-filled steel tubes in a fire situation – Numerical model and the "air-gap" effect

Pilares curtos compostos por tubos de aço preenchido com concreto em situação de incêndio – Modelo numérico e efeito do "air-gap"

Fábio Masini Rodrigues[a]
Armando Lopes Moreno Júnior[a]
Jorge Munaiar Neto[b]

[a]Universidade de Campinas – UNICAMP, Department of Structures, Campinas, SP, Brasil.
[b]Escola de Engenharia de São Carlos – ESC, Universidade de São Paulo – USP, Department of Structural Engineering, São Carlos, SP, Brasil.

Received 10 January 2021
Accepted 18 October 2021

Abstract: The increase in temperature reduces the strength of steel and concrete, in such a way that it is essential to verify concrete-filled steel tube columns in fire situations. Numerical simulations, with lower costs than laboratory tests, have great importance in checking resistance and defining simplified methods for design practice. However, peculiarities of the thermal and mechanical behavior of heated confined concrete and the air-gap effect (a phenomenon inherent to concrete-filled steel columns) must still be better understood. Therefore, this study presents the development of a numerical model performed in the ABAQUS software (Dassault Systemes SIMULIA Corp., 2014) for the thermomechanical analysis of short columns composed of circular and square concrete-filled steel tubes considering the air-gap effect. The air-gap phenomenon is presented and analyzed according to possibilities of implementation to the numerical model and, finally, the proposed numerical model is validated with experimental results presented in the literature. According to the study results, the numerical model can be used to define and adjust simplified methods for verification of composite columns in fire situation. The importance of considering the air-gap effect in numerical modeling was confirmed, taking into account that disregarding its effect may result in overestimated responses of the steel tube resistance in fire situations. Moreover, it was suggested thermomechanical joint analysis and the use of the explicit solver as a strategy to minimize processing time.

Keywords: composite column, fire, numerical model.

Resumo: A verificação da resistência ao fogo de pilares tubulares preenchidos com concreto é necessária, uma vez que há uma drástica redução na resistência do aço e do concreto com a elevação da temperatura. A simulação numérica, com inquestionáveis vantagens econômicas em relação aos ensaios em laboratório, tem grande importância na verificação da resistência e na definição e ajustes de modelos analíticos para uso na prática de projeto. Entretanto, parâmetros intervenientes como o comportamento térmico e mecânico do concreto confinado quando aquecido ou mesmo do chamado "air-gap", fenômeno inerente a pilares de aço preenchidos com concreto quando aquecidos, ainda carecem de melhor aprofundamento quanto à modelagem numérica. Para tanto, neste trabalho, apresenta-se o desenvolvimento de um modelo numérico no software ABAQUS (Dassault Systemes SIMULIA Corp., 2014), para análise térmico-mecânica de pilares curtos compostos por tubos de aço de seção circular e quadrada, preenchidos com concreto, considerando o efeito do"air-gap". O fenômeno do "air-gap" é apresentado e discutido em função das possibilidades de implementação no modelo numérico e, por fim, o modelo desenvolvido é validado por meio de resultados experimentais retirados da literatura. Com base nos resultados obtidos, se conclui que o modelo numérico pode ser utilizado para avaliação, ajustes e desenvolvimento de processos simplificados para verificação de pilares mistos em situação de incêndio; sendo recomendada a análise conjunta térmico-mecânica e a utilização do solver explicit como estratégia para minimizar o tempo de processamento. Aimportância da consideração

Corresponding author: Fábio Masini Rodrigues. E-mail: fabiosecfmr@gmail.com
Financial support: None.
Conflict of interest: Nothing to declare.
Data Availability: the data that support the findings of this study are available from the corresponding author, FMR, upon reasonable request.

do efeito do "air-gap" foi confirmada e desprezar o seu efeito pode resultar em avaliação superestimada da capacidade resistente do tubo de aço em situação de incêndio.

Palavras-chave: pilare misto, fogo, modelo numérico.

How to cite: F. M. Rodrigues, A. L. Moreno Júnior and J. Munaiar Neto, "Short columns composed of concrete-filled steel tubes in a fire situation – Numerical model and the "air-gap" effect," *Rev. IBRACON Estrut. Mater.*, vol. 15, no. 3, e15309, 2022, https://doi.org/10.1590/S1983-41952022000300009

1. INTRODUCTION

The columns composed of tube filled with concrete have proved to be an interesting structural solution in combining the benefits of both materials, including with regard to fire resistance [1], [2] and their use can be observed in buildings and bridge structures [3]–[5].

However, with the drastic reduction in the strength of steel and concrete with elevated temperature, further studies are needed to mitigate the possibility of accidents of catastrophic proportions.

Numerical tests are of great importance to chevk the resistance of structural members in a fire situation and in defining and adjusting simplified methods to design practice, reducing the need for many experimental tests, examples that can be found in the literature [6]–[9]. Furthermore, normative references refer to numerical models without deepening and detailing the parameters for the development of the numerical model, as verified in eurocode standards and Brazilian standards [10], [11].

The effect called air-gap occurs in columns composed of steel tubes filled with concrete when heated and consist in the formation of a gap between the steel tube and the concrete. The air-gap is basically formed by the expansion of the cross section, which occurs differently for steel and concrete, due to the properties of each material. The intensity of the axial force and the concrete shrinkage can contribute to the gap formation even before heating. Some numerical and experimental studies have been developed to simulate the effect of air-gap [8], [12], [13]. However, difficulties presented in the literature, such as the precision in determining material properties and modeling parameters, the complexity of representing the behavior of concrete at high temperatures, the movement of the water flow contained in the concrete, among others, make the phenomenon still uncertain.

The radiation heat transfer mechanism must be considered in the steel-concrete interface, since disregarding it leads to less accurate models. However, the adoption of wrong values of emissivity can deviate the results of the numerical models from those experimentally investigated [14].

Ghojel [15] carried out studies on the air-gap effect and presented tests with circular concrete-filled steel tubes specimens, heated in an electric oven to the temperature of 900 °C. The author describes that at the steel-concrete interface, joint thermal conductance (h_j) can be considered as the sum of contact thermal conductance (h_c) and the gap thermal conductance (h_g). Moreover, he describes that as the temperature of the steel increases, the conductance in the interface decreases.

To obtain more realistic temperature fields, the researcher highlights the importance of determining the conductance in the steel-concrete interface, considering the thermal conductivity of the air and the width of the gap that is formed between the steel tube and the concrete. When the steel temperature exceeds 200 °C, the water contained in the concrete, which migrated to the steel-concrete interface, has already evaporated, thus little interfering in the thermal conductivity in this interface. As the gap increases, the thermal conductivity at the steel-concrete interface decreases; however, the heating of water vapor generates an increase in its thermal conductivity, which causes an increase in thermal conductivity in the steel-concrete interface.

This paper presents a three-dimensional numerical model developed in the ABAQUS software (Dassault Systemes SIMULIA Corp., 2014) [16], to perform the thermomechanical analysis of short columns composed of concrete-filled steel tubes of circular and square sections. As an alternative for specific heat transfer analyses, a two-dimensional model was developed aiming at reducing computational effort, maintaining parity with the results obtained from the three-dimensional model.

To propose the numerical model, the types of modeling employed, and the effect of air gap were evaluated. Despite interfering in the thermal response, according to Hong & Varna [17], this effect is traditionally neglected in numerical models of columns filled with concrete and, until then, such simplification is considered conservative in columns without fire protection. Finally, the proposed numerical model was validated based on experimental results from the literature.

2. NUMERICAL MODELING

2.1 Development and parameterization of the numerical model

The numerical model presented in this paper was developed using the ABAQUS code, with transient thermal analysis and mechanical analysis (stress-strain) performed simultaneously in the same model. The specimens considered in this study consist of 500-mm high short columns composed of steel tubes filled with concrete of circular and square sections. The initial parameters were chosen based on the bibliographic references presented in the present study, as follows:

i. For three-dimensional models, meshes with the C3D8 element were used (Figure 1). The mesh refinement adopted consists of two or three elements along the thickness of the tube, depending on the thickness of the tube. For the concrete core, the finite element adopted has an area between 7% and 9% of the cross-sectional area. Along the height of the column the length of the elements was set to 10% of the column length.

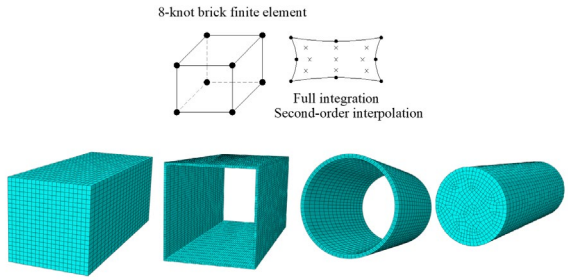

Figure 1. Refinement and type of element and mesh in the steel tube and concrete core.

A sensitivity study was performed with the three-dimensional models to define the mesh refinement required . The study was carried out considering four columns, two with circular sections and two with square sections. Two external dimensions were modeled, 14-5 mm (tube external dimension - tube thickness) equal to, and 200-8 mm. The analysis was developed with the implicit solver. Table 1 and Figure 2 show the results of the square section column with dimensions of 200-8 mm. The refinement adopted was one whose answers practically do not change in relation to an immediately superior refinement.

Table 1. Mesh sensitivity study (specimen - PQ200-8)

fire exposure time	Mesh 1		Mesh 2		Mesh 3 - adopted	
	Temperature (ºC)					
	Tube	Core	Tube	Core	Tube	Core
30 min.	698.5	95	702.4	76.6	702.4	76.7
	Axial displacement (mm)					
	1.49		1.31		1.31	
	processing time (minutes)					
	102		206		127	
50 min.	Temperature (ºC)					
	854.6	299.7	854.9	276.9	854.8	277.1
	Axial displacement (mm)					
	22.72		21.79		21.80	
	Processing time (minutes)					
	162		307		189	

PQ - square section, 200 mm of external diameter of the tube and 8 mm of thickness of the steel tube.

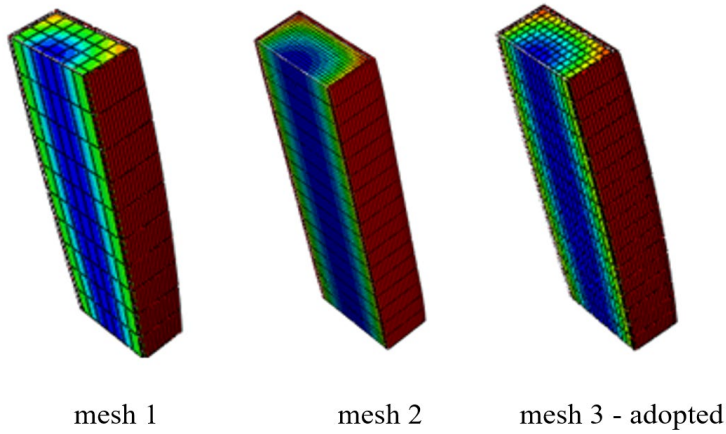

Figure 2. Finite element mesh density levels.

ii. The emissivity resulting from the exposed face of steel and fire was adopted equal to 0.7 [18], [19]; and in the steel-concrete interface, the emissivity of steel and concrete was set at 0.32 and 0.97, respectively [12].
iii. The Stefan-Boltzmann constant is expressed by the constant value equal to 5.67×10^{-8} $Wm^{-2}K^{-4}$.
iv. The convection coefficient is equal to 25 $W/m^{2}°C$ for the standard fire curve, expressed by the equation: $\theta = 345 \log(8t+1) + 20$ °C, where θ is the temperature of hot gases in the burning environment in degree Celsius and t, the time of exposure to fire in minutes [20].
v. Fire action was uniformly considered around the entire exposed surface of the column, and the initial temperature of the element/specimen was set at 20 °C.
vi. The axial force applied to thermomechanical models was set at 50% of the plastic capacity of the section at room temperature, equal to $N_{pl,Rd} = A_{afy} + A_{cfc}$, where: A_a is the cross-sectional area of steel; f_y is the yield strength of steel; A_c is the cross-sectional area of concrete; and f_c is the compressive strength of concrete.
vii. The mechanical behavior in the steel-concrete interface connection was defined by a hard contact that allows the separation between the different surfaces and does not allow overlap between them, and by a penalty contact, considering the Coulomb law with a constant coefficient of friction equal to 0.3 (in the literature this value is reported between 0.2 and 0.3) [21].

Figure 3 shows the geometry of the composite column, consisting of a steel tube filled with concrete, which is positioned inside the steel tube and connected to it by hard and penalty surface contacts method.

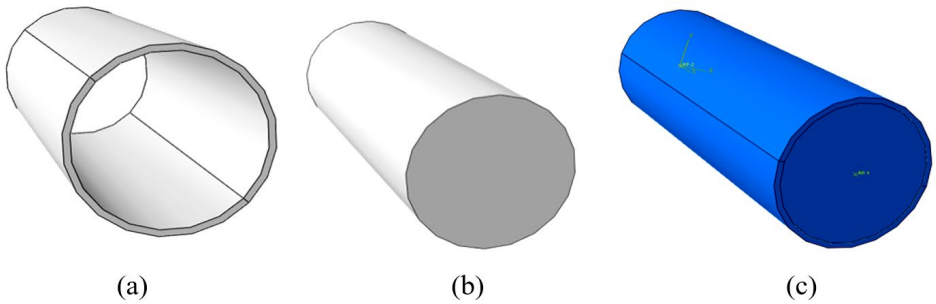

Figure 3. Schematization: (a) steel tube, (b) concrete core, and (c) complete model.

viii. The model used to simulate the concrete behavior was the CDP (Concrete Damage Plasticity), which considers the Drucker-Prager model [22], including the von Mises yield criterion, for verifying the hydrostatic pressure effect on the shear strength of the material [23]. The values of the parameters used to characterize the model were: dilatancy angle $\psi=35°$; ratio of initial equibiaxial compressive yield stress to initial uniaxial compressive yield stress σ_{bo}/σ_{co} =1.16;

eccentricity ρ=0.1; ratio between the distance from the hydrostatic axis in the deviatoric plane K_c=2/3; viscosity parameter μ=0 [8], [16], [21].

ix. The two-dimensional model run with the *static-implicit* solver and the three-dimensional model runs with the *dynamic-explicit* solver. Although the response obtained from the explicit solver is considered as an approximation, the *dynamic-explicit* method leads to a significant reduction in computational effort and to the stability of the analysis [24], [25].

2.2. Properties of steel and concrete at elevated temperatures

2.2.1. Physical and thermal properties of steel and concrete

The thermal conductivity, density, thermal expansion and specific heat of steel and concrete at high temperatures were determined from the equations described in EN 1994-1-2 (2005) [10]. The moisture contained in the concrete is usually represented by the peak value of the specific heat that ranges between 100 °C and 115 °C, linearly decreasing between 115 °C and 200 °C. After 200 °C, the values obtained for dry concrete is assumed. The peak value is indicated for 2020 and 5600 J/kgK, respectively, with 3% and 10% of moisture content. The equivalent area model was also tested to represent the specific heat proposed by Rush [13], however, there were few differences in the thermal response of the model.

2.2.2. Mechanical properties of steel and concrete

The modulus of elasticity of steel at elevated temperature ($E_{a,\theta}$), in MPa, is defined according to the Equation 1, where $K_{Ea,\theta}$, reduction factor of the modulus of elasticity of steel at elevated temperature indicated by EN1994-1-2 (2005) [10] and E_a is the steel elastic modulus at room temperature, equal to 210,000 MPa.

$$E_{a,\theta} = k_{Ea,\theta} \cdot E_a \tag{1}$$

The steel stress-strain constitutive law was defined according to the equations presented in Eurocode EN1994-1-2 (2005) [10]. The Poisson's ratio of steel is adopted equal to 0.3, regardless of temperature.

Compressive strength of concrete at high temperatures is defined by a reduction factor ($K_{C\theta} = \frac{f_{C\theta}}{f_C}$), according to the indicated normative reference and showed in Figure 4. The tensile strength of concrete at high temperatures is defined similarly, considering a reduction factor ($f_{Ck,t\theta} = K_{C,t\theta} \cdot f_{Ck,t}$).

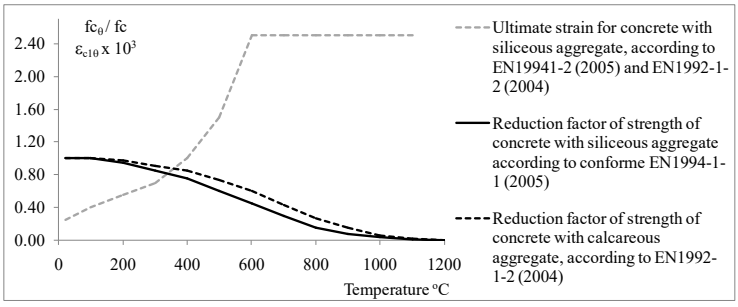

Figure 4. Reduction of compressive strength of concrete as function of temperature.

The compressive strength of concrete at elevated temperature is represented in Figure 5 and is expressed according to Equation 2 and to EN 1994-1-1 (2005) [10].

$$\boldsymbol{\sigma_{c,\theta}} = \frac{3\varepsilon_{c,\theta} f_{c,\theta}}{\varepsilon_{c1,\theta}\left[2+\left(\frac{\varepsilon_{c,\theta}}{\varepsilon_{c1,\theta}}\right)^3\right]} \tag{2}$$

Where: $f_{c,\theta} = K_{C,\theta} \cdot f_c$;$K_{c,\theta}$, reduction factor for the compressive strength of concrete; f_c = compressive strength of concrete at room temperature; $f_{c,\theta}$ = compressive strength of concrete at temperature (θ) expressed in MPa; $\boldsymbol{\varepsilon_{c1,\theta}}$ = strain corresponding to the ultimate strength of concrete at temperature (θ). The notation $\varepsilon_{c1,\theta}$ is presented in EN1992-1-2 (2004) [26], however, in EN1994-1-2 (2005) [10] it is denominated as $\varepsilon_{cu,\theta}$.

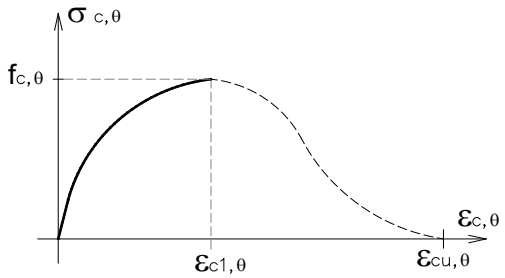

Figure 5. Stress-strain relationship of concrete at elevated temperature.

The reduction factor of the elasticity modulus of concrete at elevated temperature is determined based on the ratio presented in Equation 3, according to EN1992-1-2 (2004) [26], where ε_{c1} is the strain corresponding to concrete at room temperature. The Poisson's ratio of concrete is indicated with a value equal to 0.2, regardless of temperature.

$$K_{Ec,\grave{e}} = K_{C,\grave{e}} \cdot \frac{\mathring{a}_{c1}}{\mathring{a}_{c1,\grave{e}}} \tag{3}$$

3. "AIR-GAP" EFFECT AND ITS IMPLEMENTATION IN THE NUMERICAL MODEL

The main objective of the study on the air gap is to conceptually present the phenomenon, to implement it in the numerical model, and to verify its influence in the evolution of the temperature field in the specimens considered in the present research.

3.1. Phenomenon description

In columns composed of steel tube filled with concrete in fire situation, the steel tube heats and expands faster than concrete, because the steel has a thermal conductivity greater than the concrete. This differential expansion forms a gap between the two elements, which is usually filled with water and air up to 200 °C, temperature at which the water vaporizes, so only the air remains (Figure 6).

The air-gap layer at the steel-concrete interface provides thermal insulation, which reduces heat transfer at the interface, that mainly occurs by conduction. Air, which has lower thermal conductivity than steel and concrete, provides resistance to the transfer of thermal energy, thus increasing the temperature in the steel tube and decreasing it in the concrete. The air gap formation depends on the tube dimensions, temperatures of steel and concrete, thermal properties of the materials, and on the stress level of the column due to the axial force load. Therefore, it is difficult to precisely determine the temperatures and the gap that is formed in the steel-concrete interface [27]. The air gap is characterized by the distance (*d*), between surface of the tube and surface of the concrete core, represented by nodes 1 and 2, with temperatures θ_1 and θ_2 (Figure 5).

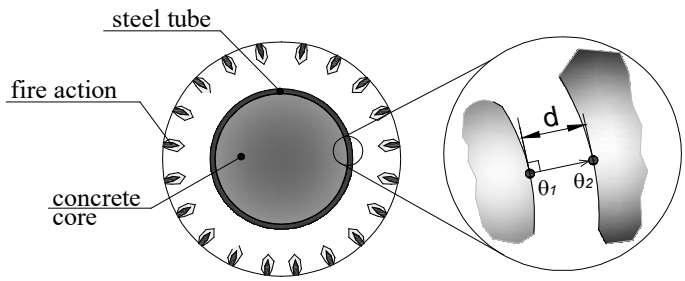

Figure 6. Gap between the two surfaces.

The gap between the concrete and the steel tube can also be formed prior to the heating of the element by the phenomenon of concrete shrinkage. In this situation, the thermal conductance at the steel-concrete interface is affected, changing temperatures and the gap formation as temperature increases. Heat transfer through the air gap can be defined by the sum of the air conductivity and the radiation between the two surfaces [28], with thermal equilibrium described as: $q = q_{ar} = q_c + q_r$.

3.2. Implementation in numerical models

To consider the air-gap effect on the numerical models developed in the ABAQUS software, a variable thermal conductivity value can be defined in the steel-concrete interface depending on the distances between the contact points. For example, the heat transfer between surfaces in contact is defined by Equation 4, where: q = heat transfer between nodes 1 and 2; h = conductivity coefficient (W/m^{2}K,); θ_1 and θ_2 are the temperatures corresponding to nodes 1 and 2.

$$q = h(\theta_1 - \theta_2) \tag{4}$$

Considering thermal equilibrium at the steel-concrete interface, Equation 4 can be described according to Equation 5. In a fully coupled thermomechanical analysis it is possible to approximate Equation 5 by considering finite differences in a subroutine, which is solved in each increment time defined in the analysis [28].

$$h(\theta_1 - \theta_2) = \frac{\lambda_{ar}}{d} + \left(\frac{1}{\varepsilon_1} + \frac{1}{\varepsilon_2} - 1\right)^{-1} \sigma\left(\frac{\theta_1^4 - \theta_2^4}{\theta_1 - \theta_2}\right) \tag{5}$$

In equation 5 the symbol λ_{ar} represents the thermal conductivity of the air.

In the model, the distance between the steel tube and the concrete (*d)* is determined by the thermomechanical analysis; deformations of each point on each surface in contact are obtained from each iteration step, and so are temperatures $\theta_1$and θ_2. Emissivity of surfaces ($\varepsilon_1$and ε_2) and air conductivity (λ_{ar}) are parameters difficult to determine, and the adoption of inconsistent values can produce very inaccurate responses. In addition to difficulties in determining the resulting emissivity and air properties, another aspect worthy of consideration is the computational complexity and time to solve the model, with several interactions in a highly nonlinear and interdependent system, with great possibility of convergence problems in the analysis [13].

An alternative approach to consider the air-gap effect is to define a thermal resistance in the steel-concrete interface by defining a calibrated thermal conduction value at this interface. The mentioned thermal conductance can be defined by an average and constant value or as a function of temperature, in such a way that the effect is like the air-gap effect, which suggests the need for experimental evaluation. The adoption of a thermal resistance in the tube-concrete interface can be easily implemented in exclusively thermal models and can also be used in thermomechanical models.

In the analyses with two or three-dimensional numerical models, the air-gap effect can be considered with the inclusion of a coefficient of thermal conductance, according to Equation 6 proposed by Ghojel, 2004 [15], where: *hj* is the joint thermal conductance at the steel-concrete interface (W/m^{2}K); θ_a is the temperature of steel in Celsius degree.

$$h_j = 160{,}5 - 63{,}8exp\,(-339{,}9{\theta_a}^{-1{,}4}) \tag{6}$$

Ghojel [15] also defined a specific equation for situations in which the column is not subjected to an axial force. However, Equation 3 can be used for both situations, with and without the presence of axial force, considering that the existence of axial force, in actual design situations, causes small changes in the temperature field [29]. Considering the joint thermal conductance at the steel-concrete interface (*hj*), according to Ghojel, 2004 [15], the heat flux (*q*) is defined by Equation 7.

$$q = hj \cdot \Delta\theta \tag{7}$$

3.3. Models with the air layer explicitly modeled

A reference model was developed considering the effective modeling of an air layer placed between the steel tube and the concrete core, to evaluate the accuracy of the thermal behavior response with the assumptions usually adopted

to consider the air gap in the numerical models. The study initially describes the properties of air, as reported in the literature, and then presents the model with the air layer and other models with assumptions usually adopted in numerical modeling.

3.3.1. Air properties

Air´s properties found in the literature are usually obtained from experimental tests and indicated with values: density = 1225 kg/m^3; specific heat = 1000 J/kg·K; elasticity modulus = 1.42 x 105 Pa; Poisson's ratio = 0; thermal conductivity = 0.023 W/m^{2}K and convection = 8 W/m^{2}K [14].

The specific heat of the air is presented in the literature as a function of temperature, with values varying from 1007 to 1234 J/kgK [30]; the density of the air ranges from 1204 to 199 kg/m^3; and the air conductivity, from 0.025 to 0.1 W/mK, which are limit values described for temperatures of 20 and 1500 °C [30], respectively. In Figure 7 the graphs represent the air density, specific heat and thermal conductivity.

The thermal conductivity of the air is also reported in the literature with different values and considering two literature references [14], [30], the conductivity of the air is expressed according to Figure 7. Conversely, the continuous line expresses the values determined by the least squares between the functions compiled from the literature, and its equation was used to define the values of the thermal conductivity of the air adopted in the numerical models.

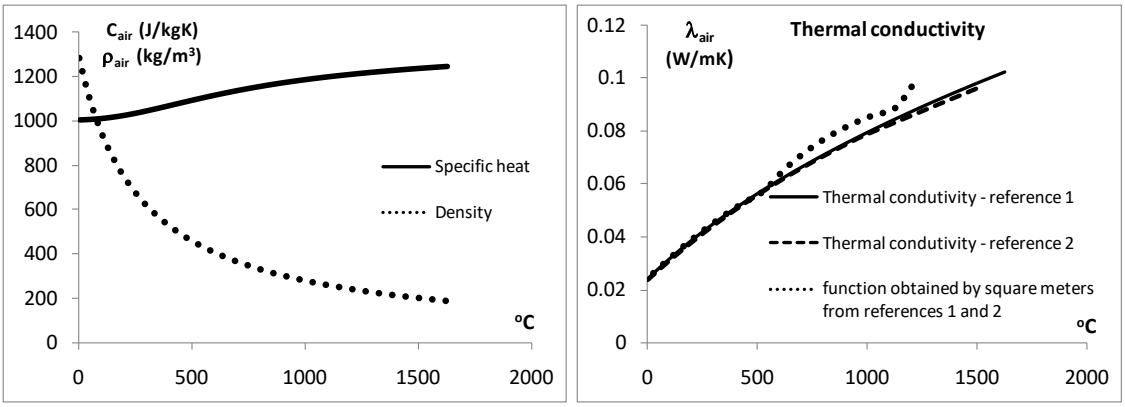

Figure 7. Density, specific heat and thermal conductivity of the air.

By adjusting the graphs to a maximum error of 5%, Equations 8 and 9 were defined to describe the thermal conductivity of the air (W/mK) and the specific heat of the air (J/kgK).

$$\lambda_{ar} = -12{,}78 \times 10^{-9}\theta^2 + 6{,}75 \times 10^{-5}\theta + 2{,}52 \times 10^{-2} \quad (8)$$

$$C_{ar} = -5{,}1 \times 10^{-5}\theta^2 + 0{,}244\theta + 987 \quad (9)$$

In the model with the effective air gap layer, equation 10 was used. The equation describes the air density (kg/m^3) and was obtained in the present work by correlation, where: φ is the temperature in °C.

$$\rho_{ar} = 55.5 \times 10^{-5}\theta^2 - 1{,}15\theta + 1000 \quad (10)$$

3.3.2. Effective modeling of the air gap

To identify and evaluate the air-gap effect, a three-dimensional model was developed with heat transfer analysis considering the air layer between the steel tube and the concrete, modeled using solid elements. The evaluation was carried out in the three-dimensional specimens shown in Table 2, with a 4% moisture content in the concrete.

Table 2. Specimens for the model with heat transfer analysis.

Reference	Cross Section	D (mm)	t (mm)	l (mm)
1. PC-168-6	Circular	168.3	6.4	500
2. PC-168-10	Circular	168.3	10	500
3. PC-300-10	Circular	300	10	500
4. PC100-6	Circular	100	6	500
5. PC-168-16	Circular	168.2	16	500
6. PC-200-6	Circular	200	6	500
7. PC-200-16	Circular	200	16	500
8. PC-500-6	Circular	500	6	500
9. PC-500-16	Circular	500	16	500
10. PC-100-6	Circular	100	6	500

D - Outer diameter of circular section; t - tube thickness; l - tube length

The evaluation of the behavior of specimens indicated in Table 2 with the air layer effectively incorporated into the model was assessed considering the air layer thicknesses of 0.5 mm, 1.0 mm and 2.0 mm. Figure 8 shows the temperature field, obtained from specimen 1. Model (a) and (c) consider the perfect thermal contact; and model (b) and (d) considers the gap effectively filled with air, both for the same fire exposure times from the ISO-834-1999 curve [20].

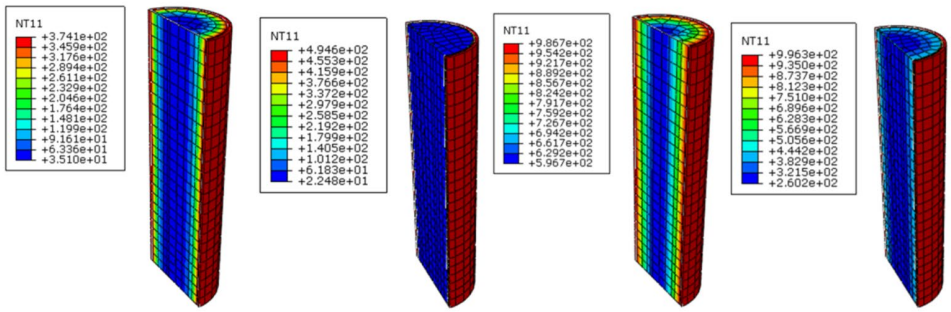

Figure 8. Models for assessing the air-gap effect: (a) perfect thermal contact (15 min.), (b) with air-gap layer of 2-mm thickness (15 min.), (c) perfect thermal contact (90 min.) and (d) with air-gap layer of 2-mm thickness (90 min.)

In Figure 9, the responses of models are presented considering specimen 4, with a thickness of 1.0 and 2.0 mm for the modeled air layer, response of model with perfect thermal contact and response model with thermal resistance proposed by Ghojel, 2004 [15].

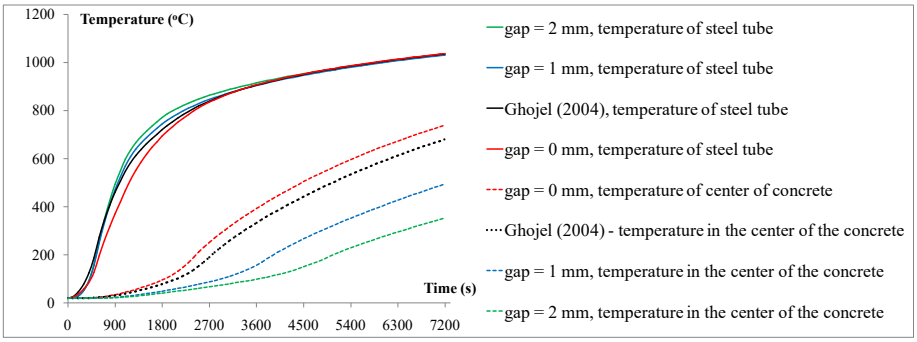

Figure 9. Temperature evolution according to the thickness of the air-gap layer.

From the models indicated in Table 2, the sensitivity of the model was verified considering differences in air properties, as reported in the literature [14], [30] and considering the inclusion of the combined properties of air and water, remembering that the gap may contain water and air. The air gap was considered with thicknesses of 0.2, 0.5, 1.5, and 3.0 mm. The models were also developed without the air layer and with the thermal resistance in the steel-concrete interface, imposed by the thermal conductance values conveniently adopted. To define the thermal conductance and, in turn, the thermal resistance at the steel-concrete interface, some alternatives were modelled, namely, model 1 according to the equation presented by Ghojel [15]; model 2 with thermal resistance constant value ranging between 100 and 200 m^2K/W; model 3 with air layer effectively modeled with the thermal conductivity equal to 0.024 W/mK; model 4 with the air layer effectively modeled with the thermal conductivity as function of temperature (Equation 8); model 5 with the air layer effectively modeled considering Equation 8, except for temperatures ranging from 0 to 200 °C when the mean value between air conductivity and water conductivity was set at 0.6 W/mK. Figures 10 and 11 show the results concerning the specimen 4.

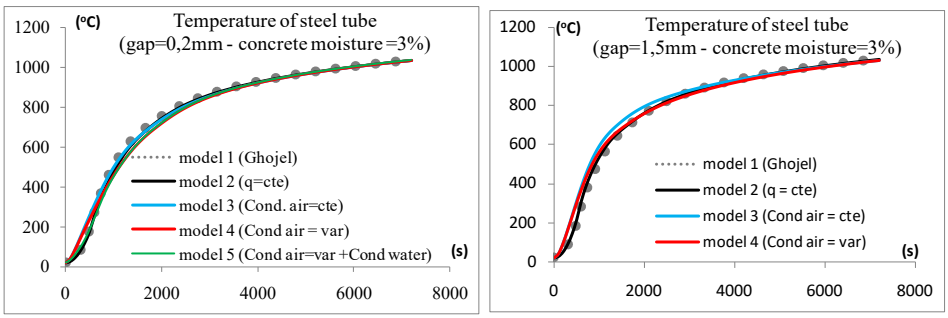

Figure 10. Temperature of steel tube according to the gap (3% concrete moisture).

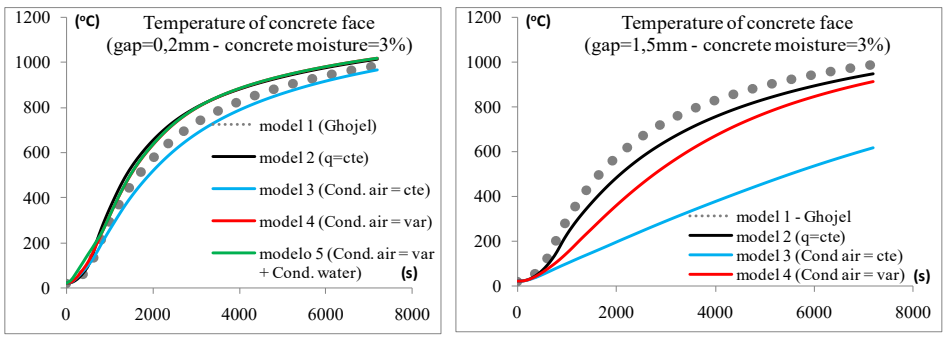

Figure 11. Temperature of concrete face according to the gap (3% concrete moisture).

Shrinking concrete can result in an initial gap before heating the element, between the steel tube and the concrete filling. Considering this effect, it is observed that the evolution of the gap with increased temperature is significantly amplified (Figure 12).

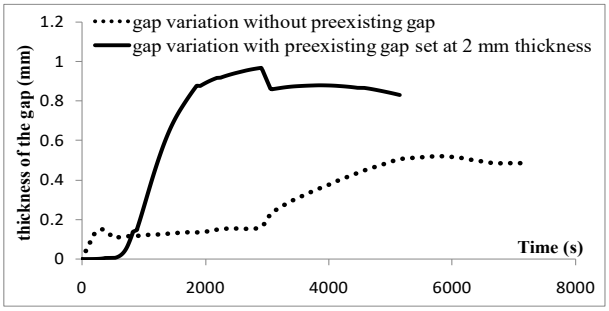

Figure 12. Evolution of the gap in the steel-concrete interface, considering an initial gap.

Assessing the result it can be observed that, (a) considering the constant value of the thermal conductivity of the air, temperatures were higher in the steel tube and lower in the concrete face, compared with the models with the air conductivity as a function of temperature; (b) from a practical point of view, the adoption of the thermal conductivity of the air with the presence of water has little influence on the evolution of temperature over the usual required fire resistance time; (c) considering a preexisting gap, prior to heating, it is verified that the development speed of the gap between the tube and the concrete significantly increases and, likewise, the temperature in the steel considerably increases, though reducing the temperatures in the concrete.

3.4. Air-gap effect modelled as equivalent to the thermal energy transfer resistance

The evaluation of the effect of thermal resistance between the steel tube and the concrete core was performed by comparing the temperature fields obtained from the numerical models of the specimens indicated in Table 2, considered in the steel-concrete interface, (a) perfect thermal contact; (b) thermal resistance according to conductance as defined by Equation 6; (c) thermal resistance considered with constant conductance values of 100 and 200 m^2K/W. Figure 13 shows the model responses for specimen 7.

According to Figure 13 it was observed that responses with the formulation proposed by Ghojel [15] have a similar behavior compared with models that adopted a constant value for thermal resistance, ranging between 100 and 200 W/m^2K. In this analysis, the axial force was fixed at 50% of the plastic capacity at room temperature.

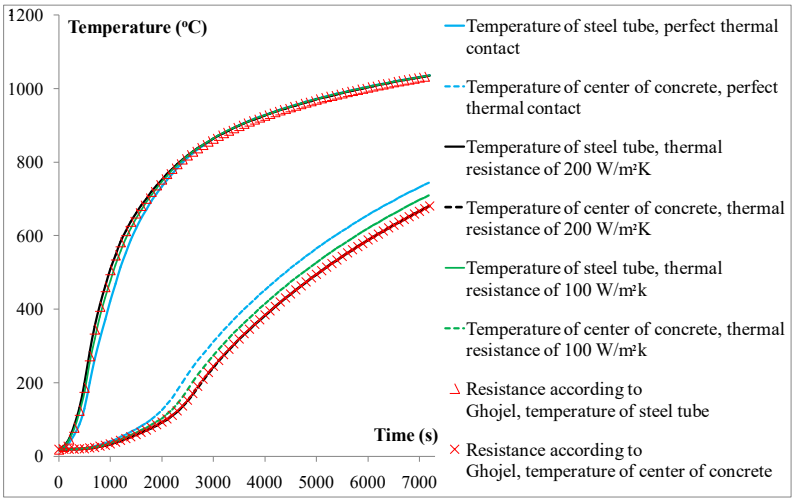

Figure 13. Temperature vs. time, according to thermal resistance tube-concrete interface.

Figure 14 graphs show the evolution of the gap and temperature in the steel tube and in the center of the concrete core for the model of specimen 7.

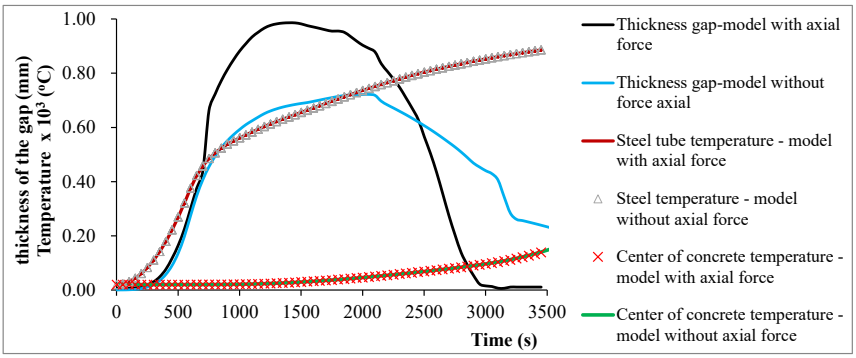

Figure 14. Evolution of the gap and temperature over time.

Based on the studies performed, the consideration of the axial force in the column altered the thickness of the gap in the tube-concrete interface; however, the resulting temperatures in the steel tube and in the concrete remained virtually the same. Experimental tests developed by Kado [29] also demonstrated a small influence on the temperature field with the application of axial force to concrete-filled steel columns.

4. VALIDATION OF THE PROPOSED MODEL

To verify the accuracy of the numerical model including the air-gap effect, its results were compared with the experimental results presented in the literature. Related to exclusively thermal analyses, a two-dimensional model was used. The specimens were modeled with the same properties as the experimental specimens.

4.1. Three-dimensional model

For the thermomechanical analysis proposed in the present study, a pinned support at the base of the column was imposed in the model, while a rigid adiabatic surface was defined at the top of the column (Figure 15), without its own weight, to improve the axial force transfer to the steel and concrete core, avoiding problems of stress concentration and convergence in the analysis.

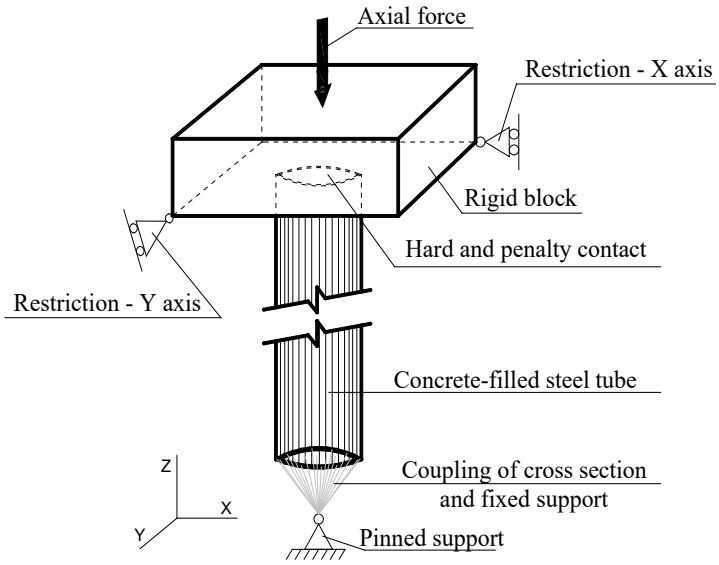

Figure 15. Boundary conditions and interactions imposed in the model.

Figure 16 presents the models in ABAQUS, with deformations that occur in response to the axial force applied to the top of the rigid surface and in response to heating, whose isotherms in the longitudinal section can be observed in the figure (c).

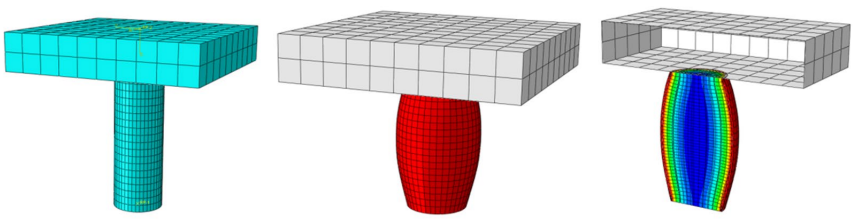

(a) (b) (c)

Figure 16. Schematization: (a) numerical model, (b) corresponding axial deformation, and (c) temperature field.

The validation models considered three specimens experimentally tested and reported in the literature, whose characteristics are indicated in Table 3.

Table 3. Characteristics of specimens and experimental results.

Reference/ specimens	Cross Section	L or D (mm)	t (mm)	fc (MPa)	f_{ys} (MPa)	l (m)	Axial force kN	FRT (min.)
1- PC 159-3.6	Circular	159	3.6	34	289	0.80	335	28
2- PQ 200-4.5	Square	200	4.5	28	293	1.32	293	76
3- PQ 120-2.9	Square	120	2.9	53.2	340	0.38	388	90

D- Outer diameter or L-outer edge dimension of the square section tube; FRT-fire resistance time. Reference: 1- Hass et al. [31]; 2-Suzuki et al. [32] and 3-Han et al. [33].

The parameters used in the modeling and the properties of steel and concrete were determined according to items 2 and 3 of this paper, while the steel and concrete strength were adopted equal to those described in the actual experimental tests [31]–[33].

The level of mesh refinement followed the definitions of the sensitivity study presented in this research, and the thermal resistance between the concrete and the steel tube was considered using Equation 6 proposed by Ghojel [15]. The axial force applied to each specimen numerically tested followed the force identified in the respective experimental test, as shown in Table 3. Likewise, the experimental specimens were heated with the standard fire curve. The content of water contained in the concrete was not explained in the references but was set at 5% in the numerical modelling.

To determine the capacity of the specimen numerically tested at elevated temperatures, the criterion indicated in EN 1363-1 (1999) [34] was adopted, which defines the failure limit equal to as 1% for the axial contraction and equal to 0.3%/min for the axial contraction rate.

Figure 17 show the curves of the axial displacement and the axial displacement rate for the three specimens numerically tested, verifying the fire exposure time at which the resistance capacity of each specimen reaches its limit.

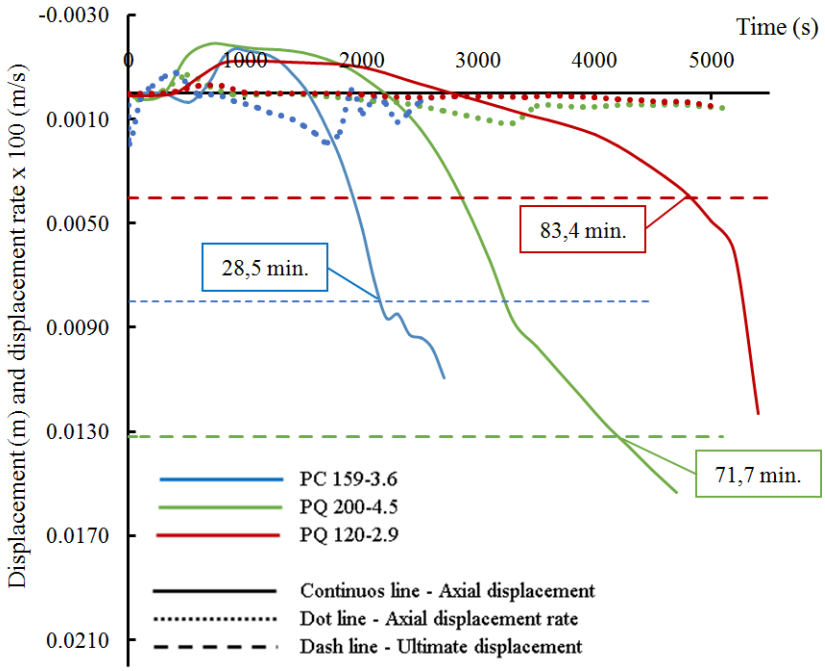

Figure 17. Fire resistance time for specimen 1, 2 and 3.

According to the response presented in the graphs, it is observed that the capacity of specimens 1, 2, and 3 (Table 3) occurs, at the times of 28.5, 71.67, and 83.4 minutes, respectively, with differences of 1.78%, -5.7%, and -7.3% from the times determined in the experimentally tested specimens.

4.2. Two-dimensional thermal analysis model

For the exclusively thermal analysis, the use of two-dimensional models is common, which results in a much less computational effort than three-dimensional models. In the present study, a two-dimensional model was presented for the analysis of heat transfer, derived from the three-dimensional model, disregarding parameters and properties of materials inherent in the mechanical analysis, considering that the thermal properties of the materials were maintained. The steel tube and the concrete core were separately modeled as two-dimensional elements and then coupled, considering the thermal resistance at the interface between tube and concrete to contemplate the air-gap effect.

The heat transfer analysis was performed with the quadrilateral D2D3 finite element for the square sections; and the three-node DC2D3 element for the circular sections. The thermal load (fire) heats the exposed face according to standard fire curve considering the convection with heat transfer coefficient equal to 25 W/m^2K and the radiation with emissivity coefficients of fire and exposed face (steel) equal to 0.7 and 1.0, respectively. The emissivity coefficient at the steel-concrete interface adopted was 0.32 and 0.97, respectively for steel and concrete. The thermal load (fire) was uniformly considered around the entire section, and the initial temperature was set at 20 ºC. The contact between the steel pipe and the concrete core was established by a “surface contact”, in which the thermal resistance is inserted to represent the air-gap effect.

Figure 18 illustrates the two-dimensional model with the temperature field established for a given time of exposure to fire.

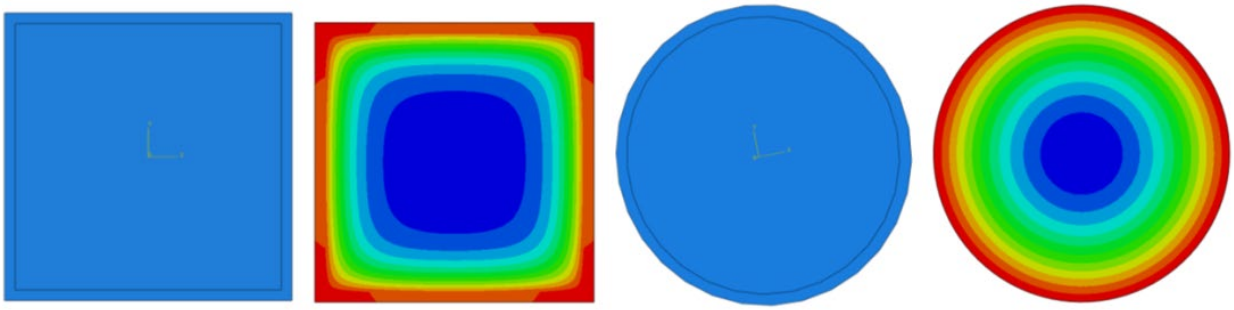

Figure 18. Illustration of the two-dimensional model with temperature fields.

The models presented next were developed to better define the numerical model demonstrated. Differences found in the response of the numerical model were effectively investigated, according to the type of analysis and adopted solver.

The validation of the two-dimensional model considered the experimental results presented by Rush [13] as reference. The specimen experimentally tested and reproduced by the two-dimensional numerical model has the following characteristics, circular section steel tube with 219.1 and 10 mm in diameter and thickness, respectively; water content in the concrete set at 6% of the concrete mass, and emissivity resulting from fire and exposed face set at 0.38, as indicated in the description of the experimental test. The properties of steel and concrete are indicated in item 3.

Table 4 describes the temperatures at the points indicated in Figure 19, as well as the percentage differences in relation to the experimental model. The results presented in Table 4 refer to specimen 1 (Table 3) and the notations “Exp.”, “1-Num.” and “2-Num.” correspond to the experimental response, response obtained by the numerical model considering the effect of air gap and response of the numerical model with perfect thermal contact between the steel tube and the concrete core, respectively.

Table 4 – Temperatures found in experimental and numerical models.

	Temperature (ºC)								
	Steel tube			External face of concrete			Center of concrete		
	30 min	90 min	120 min	30 min	90 min	120 min	30 min	90 min	120 min
Exp.	503	887	971	285	770	885	47	180	330
1-Num.	553	902	984	377	792	920	46	178	376
2-Num.	502	873	968	432	799	924	55	221	398
% Exp vs 1-Num	9.0	1.7	1.3	24.4	2.8	3.8	-2.2	-1.1	12.2
% Exp vs 2-Num	-0.2	-1.6	-0.3	34.0	3.6	4.2	14.5	18.6	17.1

Figure 19 shows the points chosen for the identification of temperatures in the cross section.

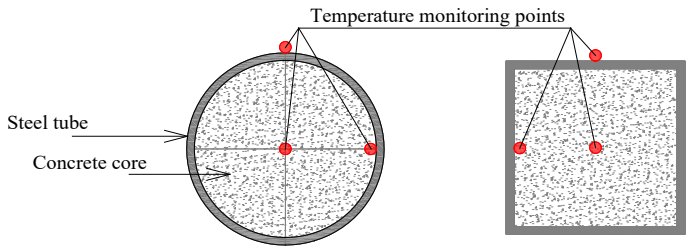

Figure 19. Monitoring points in the cross section.

Figures 20 and 21 show the temperature fields of the validation specimens indicated in Table 4 for fire exposure times of 60 and 120 minutes.

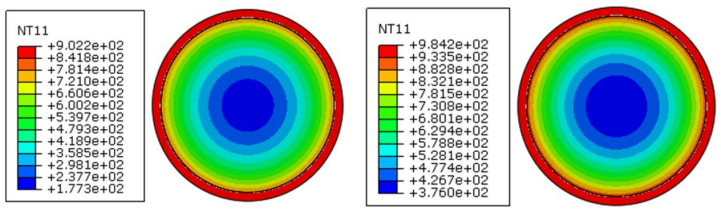

(a) fire exposure time – 60 min. (b) fire exposure time – 120 min.

Figure 20. Temperature field obtained from the numerical model with air gap

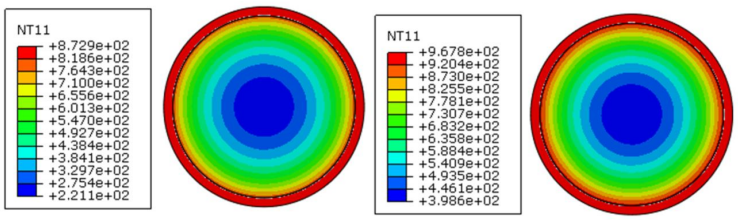

(a) fire exposure time – 60 min. (b) fire exposure time – 120 min.

Figure 21. Temperature obtained from the numerical model with perfect thermal contact

5. CONCLUSIONS

The presented three-dimensional models and the two-dimensional model, the last being exclusive to heat transfer analysis, provided results close to experimental tests reported in the literature. The two-dimensional model used for specimens of symmetrical geometry and uniform fire action proved to be an effective alternative to determine temperature fields in tubular concrete-filled columns.

The three-dimensional model with thermomechanical analysis aims on the behavior of tubular columns filled with concrete in a fire situation, yielding fire resistance time 8% smaller than the experimental result.

The inclusion of the air-gap effect, influence the temperature field and, in turn, the determination of the ultimate axial force at a given fire exposure time.

Related to heated tubes filled with concrete, the air opening formed in the steel-concrete interface behaves as a thermal insulation, influencing the heat transfer from the steel tube to the concrete core. Its inclusion in the models results in higher temperatures in the steel tube and lower temperatures in concrete, and by disregarding this effect, the temperature in steel is underestimated and the concrete temperature is overestimated. In the cases analyzed the result differences reach 25% in the temperature of the steel tube and 20% in the concrete core.

The air-gap effect can be considered as a thermal resistance in the steel-concrete interface, with thermal conductance and values established based on the equation proposed by Ghojel (Equation 6). The adoption of this equation produced equivalent results to those obtained with the inclusion of 0.1 to 0.5 mm openings filled with air in the steel-concrete interface, in the numerical models tested.

Although considering the effect of the air gap on the model, with the responses of the numerically resolved specimens close to the responses obtained experimentally, there are still uncertainties on how to define it, since the flow of water contained in the concrete can affect their behavior. Another issue is due to the possible existence of a gap between the steel tube and the concrete before heating the element and that is caused, for example, by the effect of the concrete shrinkage. This previous gap amplifies the evolution of the gap and, consequently, its effect.

Therefore, it is noteworthy the importance of considering the air-gap effect in the model and performing further research on the subject, seeking to improve the numerical and analytical procedures.

A conservative, but recommended in the present stage of knowledge, approach for the definition of practical procedures for the design of columns composed of tubes filled with concrete is to consider the thermal resistance according to the equation proposed by Ghojel (2004), to determine the temperatures in the steel tube only, neglecting the effect of the air gap to determine the temperatures in the concrete core.

The thermomechanical analysis performed in the model (coupled analysis), in which the structural limb is heated with an imposed axial force, better represents the structural behavior, considering that strains, stresses are obtained together with the formation of the temperature field

It is important to point that the use of dynamic-explicit solver in the thermal-mechanical analyses results in shorter computational processing time, avoiding convergence problems resulted with the use of the implicit solver.

A good approximation among the experimental and numerical models was obtained considering the steel and concrete properties indicated in EN1994-1-2 (2005). The model with the specific heat considering the water contained in the concrete should be improved and the model proposed by Rush [13] did not result in significant changes in the temperature field, however, this model was verified with only one specimen simulation, not enough to evaluate the proposal result.

ACKNOWLEDGEMENTS

We would like to thank University of Campinas and Universidade Católica de Santos.

REFERENCES

[1] V. R. Kodur. Guidelines for fire resistant design of concrete-filled steel HSS columns - state-of-the-art and research needs. *Int. J. Steel Struct*., vol. 7, no. 3, pp. 173-182, 2007.

[2] D. Hernández, “Estudio experimental del pandeo de perfiles tubulares retangulares de aço, rellenos de hormigón de alta resistência, bajo carga axial y diagrama de momentos variable”, Tesis Doctoral. Univ. Politècnica de València, España, 2011.

[3] M. T. Stephens, D. Lehman, and C. W. Roeder, "Seismic performance modeling of concrete-filled steel tube bridges: tools and case study," *Eng. Struct.*, vol. 165, pp. 88–105, 2018.

[4] N. K. Brown, M. J. Kowalsky, and J. M. Nau, "Impact of D/t on seismic behaviour of reinforced concrete-filled steel tubes," *J. Construct. Steel Res.*, vol. 107, pp. 111–123, 2015.

[5] S. Morino and K. Tsuda, "Design and construction of concrete-filled steel tube column system in Japan," *Earthq. Eng. Eng. Seismology*, vol. 4, no. 1, pp. 51–73, 2003.

[6] F. Sciarretta, "Modeling of mechanical damage in traditional brickwork walls after fire exposure," *Adv. Mat. Res.*, vol. 919-921, pp. 495–499, 2014.

[7] T. Nguyen, F. Meftah, R. Channas, and A. Mebarki, "The behaviour of masonry walls subjected to fire: Modelling and parametrical studies in the case of hollow burnt-clay bricks," *Fire Saf. J.*, vol. 44, no. 4, 2008.

[8] A. Espinós Capilla, "Numerical analysis of the fire resistance of circular and elliptical slender concrete filled tubular columns", Doctoral thesis, Univ. Politècnica de València, España, 2012.

[9] C. Renaud, CTICM. Report reference INSI – 04/75b – CR/PB, France, 2004.

[10] European Committee for Standardization, *Eurocode 4: Design of Composite Steel and Concrete Structures – Part 1.2: Structural Fire Design*, EN 1994-1-2:2005, 2005.

[11] Associação Brasileira de Normas Técnicas, *Fire Design of Steel Structures and Composite Steel and Concrete Structures*, NBR 14323:2013, 2013.

[12] E. O'Loughlin, D. Rush, and L. Bisby "Concrete-filled structural hollow sections in fire: accounting for heat transfer across a gap", in *Proc. 15th Int. Conf. on Exp. Mech.* (pp. 1–17). Porto, Portugal, 2012.

[13] D. Rush, "*Fire performance of unprotected and protected concrete filled steel hollow structural sections*," Doctoral thesis, University os Edinburgh, 2013.

[14] Z. G. Han and M. Gillie, "Temperature Modeling for Concrete-filled Steel Tube's Cross Section in Fire". in *Proc. Int. Conf. Mech. Civ. Eng.*, 2014.

[15] J. Ghojel, "Experimental and analytical technique for estimating interface thermal conductance in composite structural elements under simulated fire conditions," *Exp. Therm. Fluid Sci.*, vol. 28, pp. 347–354, 2004.

[16] Dassault Systemes Simulia Corp. *ABAQUS/CAE User's Guide*, 2012.

[17] S. Hong, and H. Varma, "Analytical modeling of the standard fire behavior of loaded CFT columns," *J. Construct. Steel Res.*, vol. 65, pp. 54–69, 2009.

[18] European Committee for Standardization, *Eurocode 1: Actions on Structures – Part 1.2: General Actions - Actions on Structures Exposed to Fire*, EN 1991-1-2, 2002.

[19] European Committee for Standardization, *Eurocode 3: Design of Steel Structures – Part 1.2: General Rules - Structural Fire Design*, EN 1993-1-2, 2005.

[20] International Organization for Standardization, *Fire-resistance Tests – Elements of Building Construct: General Requirements*, ISO 834-1, 1999.

[21] Rodrigues, J. P., *European Project FRISCC - Finite Element Modeling of Innovative Concrete-Filled Tubular Columns Under Room and Elevanted Temperatures*, España: Univ. Politècnica de València, 2012.

[22] D. C. Drucker and W. Pragger, "Soil mechanics and plastic analysis or limit design," *Q. Appl. Math.*, vol. 10, pp. 157–165, 1952.

[23] W. F. Chen, *Plasticity in reinforced concrete*, McGraw-Hill, 1982.

[24] D. Y. Yang et al., "Comparative investigation in to implicit, explicit, and iterative implicit/explicit schemes for the simulation of sheet-metal forming processes," *J. Mater. Process. Technol.*, vol. 50, pp. 39–53, 1995.

[25] M. F. Rodrigues and A. L. Moreno Júnior, "Análise numérica de pilares mistos curtos, através dos métodos implicit e explicit", in *Proc. 4th CILASCI*, pp. 85-98, Recife - Pernambuco, 11 out. 2017.

[26] European Committee for Standardization, *Eurocode 2: "Design of Concrete Structures – Part 1.2: General Rules - Structural Fire Design,* EN 1992-1-2, 2004.

[27] J. Ding and Y. C. Wang, "Realistic modelling of thermal and structure behaviour of protected concrete filled tubular columns in fire," *J. Construct. Steel Res.*, vol. 64, pp. 1086–1102, 2008.

[28] S. Afazov, "Modelling of thermal gap condutance in casting using finite element analysis," *Manuf. Technol. Center*., pp. 1-11, 2013. Accessed: Jan. 10, 2021. [Online]. https://www.researchgate.net/publication/262450677

[29] B. Kado, S. Mohammad, Y. I. I. Lee, P. N. Shek, and M. A. A. Kadir "Experimental investigation on temperature distribution of foamed concrete filled steel tube column under standard fire," in *Proc. IOP Conf. Ser.: Earth Environ. Sci.*, vol. 140, pp. 012136, 2018, https://doi.org/10.1088/1755-1315/140/1/012136.

[30] Shpilrain, E. E., "Air (Properties of)," *Thermopedia*, 2011, https://doi.org/10.1615/AtoZ.a.air_properties_of.

[31] R. Hass, J. Ameler, H. Zies, and H. Lorenz, *Fire Resistance of Hollow Section Composite Columns with High Strength Concrete Filling*, Brunswick: CIDECT, 2001. Final Report.

[32] T. Suzuki, M. Kimura, A. Kodaira, and M. Fushimi, "Experimental study on fire resistance of concrete filled square steel columns: structural behaviour under constant axial force in fire," *J. Struct. Constr. Eng.*, vol. 350, pp. 77–85, 1985.

[33] L. N. Han et al., "Compressive and flexural behaviour of concrete filled steel tube safe exposure to standard fire," *J. Construct. Steel Res.*, vol. 61, pp. 882–901, 2005.

[34] European Committee for Standardization, *Fire Resistance Tests - Part 1: General Requirements, EN 1363-1:1999*, 1999.

Author contributions: FMR: conceptualization, development, methodology, modeling, writing; ALMJ: conceptualization, methodological analysis, supervision and JMN: conceptualization, methodological analysis, supervision.

Editors: Bruno Briseghella, Guilherme Aris Parsekian.